# Ratiometric Pulsed Alkylation/Mass Spectrometry of the Cysteine Pairs in Individual Zinc Fingers of MRE-Binding Transcription Factor-1 (MTF-1) as a Probe of Zinc Chelate Stability†

Julius L. Apuy,‡ Xiaohua Chen,‡ David H. Russell,# Thomas O. Baldwin,‡,#,§ and David P. Giedroc*,‡

*Department of Biochemistry and Biophysics, Center for Advanced Biomolecular Research, Texas A&M University, College Station, Texas 77843-2128 and Department of Chemistry, Texas A&M University, College Station, Texas 77843-3255*

*Received June 13, 2001; Revised Manuscript Received September 14, 2001*

ABSTRACT: Metal-response element (MRE)-binding transcription factor-1 (MTF-1) is a zinc-regulated transcriptional activator of metallothionein (MT) genes in mammalian cells. The MRE-binding domain of MTF-1 (MTF-zf) has six canonical $Cys_2-His_2$ zinc finger domains that are distinguished on the basis of their apparent affinities for zinc and their specific roles in MRE-binding. In this paper, pulsed alkylation of the zinc-liganding cysteine thiolate pairs with the sulfhydryl-specific alkylating reagent $d_5$-*N*-ethylmaleimide ($d_5$-NEM) is used as a residue-specific probe of the relative stabilities of the individual zinc finger coordination complexes in $Zn_6$ MTF-zf. A chase with excess $H_5$-*N*-ethylmaleimide ($H_5$-NEM) to fully derivatize MTF-zf concomitant with complete proteolysis, followed by MALDI-TOF mass spectrometry allows quantitation of the mole fraction of $d_5$,$d_5$-, $d_5$,$H_5$-, and $H_5$,$H_5$-NEM derivatized peptides corresponding to each individual zinc finger domain as a function of $d_5$-NEM pulse time. This experiment establishes the hierarchy of cysteine thiolate reactivity in MTF-zf as F5 > F6 ≫ F1 > F2 ≈ F3 ≈ F4. The apparent second-order rate of reaction of F1 thiolates is comparable to that determined for the DNA binding domain of Sp1, $Zn_3$ Sp1-zf, under identical solution conditions. The reactivities of all Cys residues in MTF-zf are significantly reduced when bound to an MREd-containing oligonucleotide. An identical experiment carried out with $Zn_5$ MTF-zf26, an MTF-zf domain lacking the N-terminal F1 zinc finger, reveals that MTF-zf26 binds to the MREd very weakly, and is characterized by strongly increased reactivity of nonadjacent F4 thiolates. These findings are discussed in the context of existing models for metalloregulation by MTF-1.

Zinc, an essential trace element found in over 300 proteins and enzymes, plays two primary roles in biology (*1*, *2*). One is a structural role in which a coordinately saturated Zn(II) coordination complex functions to stabilize the native fold of a protein or an intermolecular protein−protein or protein−nucleic acid interface; without bound Zn(II), the conformation is usually altered and often locally unfolded and functionally inactive (*3*). Zinc finger proteins represent a prominent example of a well-understood structural role for zinc (for a review, see ref *4*). Zn(II) can also play a catalytic role, where it typically functions as a Lewis acid in activating an attacking nucleophile, e.g., a water molecule in a hydrolytic enzyme (*5*). Although Zn(II) is not unique in its ability to perform these biological roles, the bioinorganic chemistry of Zn(II) is ideally suited to carry out these functions (*6*). In particular, Zn(II) is redox-inert due to its completely filled *d*-electronic shell and is considered a "borderline" Lewis acid that enables binding to a wide range of biological ligands while adopting a range of coordination numbers (typically 4 to 6) and geometries (*7*, *8*).

All cell types possess regulatory machinery to tightly control the concentration of bioavailable zinc (*9*−*12*), although the precise mechanism of zinc toxicity remains unclear. In vertebrate cells, the metalloregulated transcriptional activator protein, metal response element (MRE)[1]-binding transcription factor-1, MTF-1, plays a central role in detoxifying high concentrations of zinc and cadmium as well as protecting cells from oxidative stress (*12*−*14*). MTF-1 binds to a *cis*-acting element(s) found in the promoters of zinc-regulated genes termed a metal-response element (MRE) (*15*) and is required for both basal and zinc-stimulated transcription of the downstream genes (*16*, *17*). MREs were first characterized in the promoters of genes encoding the abundant intracellular zinc sequestering agent, metallothionein, in mouse, rat, and human cells; more

† This work was supported by grants from the NIH (R01-GM42569 to D.P.G.; P30-ES09106 to D.H.R.), the Department of Energy (DE-FG03-95ER14505 to D.H.R.), the NSF (CHE-9629966), and the Robert A. Welch Foundation (A-1295 to D.P.G.).

* To whom correspondence should be addressed: E-mail: giedroc@tamu.edu; telephone: 979-845-4231; fax: 979-862-4718.

‡ Department of Biochemistry and Biophysics.

# Department of Chemistry.

§ Present address: University Department of Biochemistry and Molecular Biophysics, University of Arizona, Tucson, AZ 85721-0088.

[1] Abbreviations: DTNB, 5,5′-dithio-bis(2-nitrobenzoic acid); EDTA, ethylenediamine tetracetic acid; MTF-1, metal-response element (MRE)-binding transcription factor-1; Mops, 3-(*N*-morpholino)propanesulfonic acid; $d_5$-NEM, $d_5$-*N*-ethylmaleimide; $H_5$-NEM, *N*-ethylmaleimide.

10.1021/bi0112208 CCC: $20.00 
Published on Web 11/21/2001

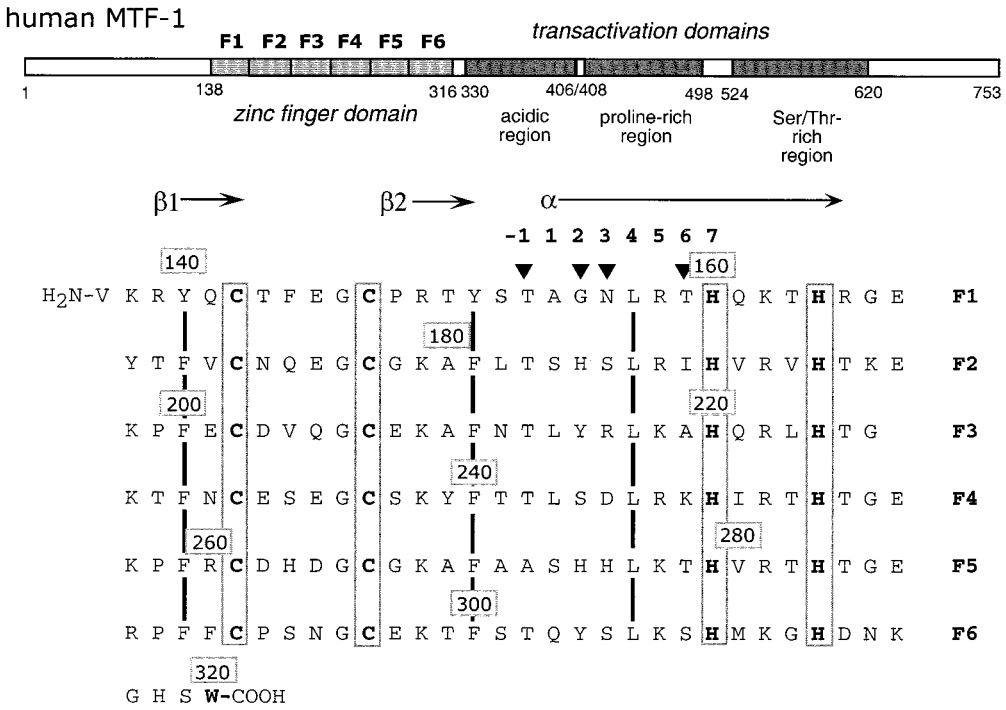


FIGURE 1: Top, schematic representation of the amino acid sequence of human MTF-1 (*14*). Bottom, amino acid sequence of the human MTF-1 zinc finger domain fragment used in these studies.

recently, functional MREs have been found in the promoters of the gene encoding ZNT1, a widely expressed zinc efflux pump (*18*, *19*), and the gene encoding $\gamma$-glutamyl-cysteine synthetase, a highly regulated enzyme in glutathione biosynthesis (*16*), as well as other target genes (*20*).

MTF-1 is a canonical TFIIIA-type zinc finger protein that contains six tandemly arrayed $Cys_2$-$His_2$ (CCHH) zinc finger domains, each of which conforms to the Cys-$\boldsymbol{X_4}$-Cys-$X_7$-His-$\boldsymbol{X_4}$-His sequence (*21*) (Figure 1). The zinc finger domain is necessary and sufficient for high affinity binding to the MRE in vitro (*22*) and in vivo (*23*). Limited evidence suggests that flanking domains do stabilize the MTF-1-MRE complex (*24*) and are required to observe Zn(II)-dependent activation of MRE binding in vitro (cf. ref *25*), but the mechanism is poorly understood. Since it is well established that tandemly arranged $Cys_2-His_2$ fingers bind to contiguous or overlapping 3−4 base pair subsites (*4*), the conserved portion of the 12-base pair MRE (*26*) is not large enough to accommodate sequence-specific recognition by all six zinc fingers in MTF-1. This has fueled speculation that the zinc fingers in MTF-1 play distinct functional roles, with a subset of zinc fingers playing a structural role in MRE-binding, with others required for Zn(II)-dependent activation of MRE binding and transcriptional activation (*25*). Recent structural and functional findings are largely consistent with this idea (*22*, *24*, *27*, *28*). Characterization of the zinc finger domain of hMTF-1, MTF-zf, showed that the C-terminal zinc finger domains, F5 and F6, played an accessory role in stabilizing the protein−DNA complex and appeared to bind Zn(II) weakly; these properties are consistent with what one might expect for metalloregulatory zinc fingers (*22*, *27*). In contrast to these expectations, functional characterization of F5 and F6 "missing-" and "broken-finger" mutants have yet to ascribe a critical role for these zinc fingers in zinc-dependent stimulation of MRE binding and transcriptional activation in vivo (*24*, *28*). On the other hand, recent functional studies were interpreted to suggest that the N-terminal zinc finger, F1, is the zinc sensor in MTF-1 (*28*).

The objective of the work described here was to gain additional insight into zinc chelate stability in zinc-saturated ($Zn_6$) MTF-zf. Previous electrospray ionization mass spectrometry experiments reveal that consensus $Cys_2-His_2$ domains bind Zn(II) such that both cysteines are negatively charged thiolate anions at neutral pH in the Zn(II) complex (*29*). Since a metal-coordinated thiolate anion is poorly nucleophilic relative to a free thiolate, a major factor that will influence the intrinsic reactivity of a metal-bound thiolate is the extent to which the coordinated Zn(II) controls the "free" thiolate via a dissociative equilibrium at the metal center (*30*, *31*). Thus, if two cysteines in otherwise identical coordination complexes, e.g., the most N-terminal cysteine in two contiguous $Cys_2-His_2$ zinc finger domains, display vastly different reactivities with an alkylating agent, this likely originates with weaker Zn(II)-thiolate bonds in one versus the other chelate (Figure 2).

In this study, we have determined the rate at which individual cysteine pairs in each zinc finger domain in MTF-zf is derivatized by the sulfhydryl-specific alkylating agent *N*-ethylmaleimide (NEM) as a probe of zinc chelate stability. Selective chemical modification and mass spectrometry have previously been used to probe protein surface topology (*32*, *33*), protein−protein interactions (*34*), protein folding (*35*) and the reactivity of cysteine ligands in metal coordination complexes toward a variety of electrophiles (*36*), including NEM (*37*). The underlying principle in these studies is that the reactivity of a specific target residue is due to the net effect of its local environment. Here, we employ selective ratiometric chemical modification, combined with protease digestion and high-resolution mass spectrometry, a method described in detail elsewhere (*38*), to determine the reactivities of cysteine thiolate pairs in individual zinc finger domains in the uncomplexed and MRE-bound forms of $Zn_6$

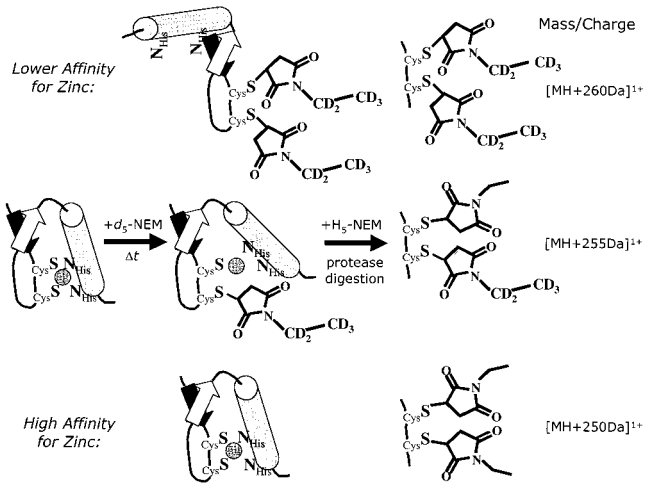


FIGURE 2: Schematic representation of the ratiometric pulsed-alkylation mass spectrometry experiment with $d_5$-NEM and $H_5$-NEM used to probe the relative stabilities of individual $Cys_2-His_2$ zinc finger-Zn(II) complexes in MTF-zf. Low affinity complexes will be characterized by increased metal−thiolate dissociation, which would make these cysteine thiolates more nucleophilic toward the aklylating reagent $d_5$-NEM, during the pulse time *t*. In contrast, cysteine thiolates in Zn(II) chelates of high stability will be refractory to modification by $d_5$-NEM and will largely become derivatized during the chase with $H_5$-NEM. The three alkylation products of the pulsed alkylation protocol, $d_5$,$d_5$-, $d_5$,$H_5$-, and $H_5$,$H_5$-NEM derivatized peptides, and their molecular masses are shown on the right.

MTF-zf at a resolution not previously possible. The results provide new insight into the solution structure, reactivity, and zinc chelate stability of individual zinc fingers in MTF-1.

## MATERIAL AND METHODS

*Materials.* Dithiothreitol was obtained from Acros-Organics, while DTNB and Mops were from Sigma. $d_5$-NEM was obtained from Medical Isotopes, Inc., while $H_5$-NEM was purchased from ICN. Trifluoroethanol was obtained from Pierce Chemical Co., while HPLC-grade acetonitrile was purchased from EM Science. Sequencing grade trypsin was obtained from Promega, while chymotrypsin was purchased from Boehringer-Mannheim. Bradykinin was obtained from Sigma.

*Purification of $Zn_6$ MTF-zf and $Zn_5$ MTF-zf26.* The zinc finger domain fragment encoding residues 137−320 of human MTF-1 (*14*) (Figure 1) denoted MTF-zf (*22*) was expressed in *Escherichia coli* BL21(DE3) and purified to homogeneity using nondenaturing conditions essentially as described previously (*22*). The MTF-zf was then exhaustively dialyzed in an anaerobic Vacuum-Atmospheres glovebox against a zinc- and dithiothreitol-free buffer containing 50 mM Mops, 0.20 M NaCl, pH 7.0. The zinc content of MTF-zf used in these experiments was determined by flame atomic absorption on a Perkin-Elmer AAnalyst 750 atomic absorption spectrometer to be 6.5 mol of Zn(II)/mol of MTF-zf, while the mol equivalents of reduced cysteines was determined to 12.4 (12 expected) by anaerobic DTNB reactivity (*38*) using $\epsilon_{280} = 16\,400\ M^{-1}\ cm^{-1}$ (*22*). MALDI-TOF revealed a mass of 21 167.3 daltons (21 167.0 daltons calculated from the amino acid sequence) A pET-based overexpression plasmid for MTF-zf26 was prepared (designated pMTF-zf26, designed to express residues 167−320 of hMTF-1), with the MTF-zf26 purified essentially as described above for MTF-zf. $Zn_5$ MTF-zf26 was found to contain 4.7 molar equivalents of Zn(II) and 9.5 (10 expected) reduced thiolates by DTNB reactivity. MALDI-TOF revealed a mass of 17 819.1 daltons (17 819.3 daltons calculated from the amino acid sequence) with an N-terminal sequence of MEYTFV(X), which matches the expected sequence of M-$^{167}$ETYFVC (*14*) (Figure 1).

*Purification of Sp1-zf.* The bacterial Sp1-zf expression plasmid, pSp1-Zn92 (*40*), was kindly provided by Professor John Caradonna (Boston University). *E. coli* BL21(DE3) transformed with pSp1-Zn92 was propagated on rich LB media at 37 °C, with the expression of Sp1-zf induced with 0.4 mM IPTG at an $A_{600}$ of 0.4 essentially as described. After 4 h, the cells were harvested by low-speed centrifugation. The wet cell paste from 9 L of cell culture was resuspended and sonicated using the methods described above for MTF-zf (vide supra). Solid urea was then added to the supernatant to a final concentration of 5.0 M, and subsequently acidified to pH 2 with HCl, with the resulting suspension centrifuged for 30 min at 12 000 rpm in a Beckman JA-20 rotor. The resulting supernatant was loaded onto a Waters Powerline HPLC system running a POROS reversed-phase C4 column (Perseptive Biosystems) equilibrated with 0.1% trifluoracetic acid (TFA) and developed with an acetonitrile gradient in 0.1% TFA. Fractions containing Sp1-zf were identified by SDS−PAGE, pooled, and then lyophilized to dryness. The dried acidified apo Sp1-zf sample was then brought into the glovebox, dissolved in a degassed zinc- and dithiothreitol-free buffer containing 50 mM Mops, 0.20 M NaCl, pH 7.0, and subjected to exhaustive anaerobic dialysis against the same buffer to create apo-Sp1-zf. Following dialysis, 3.0 molar equivalents of $ZnCl_2$ was added anaerobically. $Zn_3$ Sp1-zf prepared in this way was found to contain 3.5 (± 0.2) mol equivalents of Zn(II) and 6.0 mol equivalents reduced cysteines by DTNB reactivity.

*Purification of the MREd-Containing Oligonucleotide.* 1 μmol syntheses of crude, complementary mouse MT-I MREd-containing 23-nucleotide oligonucleotides ("top" strand: 5′-GAGCTC**TGCACTCCGCC**CGAAAA) were obtained from the Gene Technologies Laboratory at Texas A&M University. These oligonucleotides were purified by denaturing PAGE, electroeluted (S&S) from the excised gel bands, and desalted using an Alltech C-18 cartridge, as described previously (*27*). The purified complementary strands were annealed at 95 °C for 5 min in a zinc-free buffer containing 50 mM Mops, 0.20 M NaCl, pH 7.0, followed by slow cooling at room temperature. Duplex formation was confirmed by nondenaturing PAGE (data not shown).

*Ratiometric Pulsed Alkylation/Mass Spectrometry.* These methods were adapted from the original report described elsewhere (*38*). All experiments were carried out in Vacuum-Atmospheres anaerobic glovebox at ambient temperature (≈25 °C). For the MTF-zf experiments, 12 μL of 0.10 M $d_5$-NEM was added at time zero to 2.0 mL of 5.0 μM $Zn_6$ MTF-zf (60 μM cysteine thiolate; 0.6 mM $d_5$-NEM) to give a 10:1 molar ratio of $d_5$-NEM:Cys thiolate. At various times, this pulse of $d_5$-NEM reaction was terminated by withdrawing a 200 μL aliquot and adding it to a solution consisting of 12 μL of 0.10 M $H_5$-NEM, 80 μL of 0.50 M NaCl, and 2 μL of 1 mg/mL sequence grade trypsin or chymotrypsin,

to give a final 100:1 molar ratio of $H_5$-NEM:Cys thiolate (the chase contained 10:1 $H_5$-NEM:$d_5$-NEM). Three hours after the last pulse time point was taken, the proteolyzed samples were removed from the glovebox and prepared for elution from an Amika Corp. C4 microtip column. The tip columns were first wet with HPLC-grade acetonitrile, before equilibrating them with 2 mL of 0.1% TFA solution. The sample was loaded and then washed with 2 mL of 0.1% TFA solution before elution with a 0.1% TFA/100% acetonitrile solution. The sample was vacuum-centrifuged to dryness and dissolved in 50 $\mu$L deionized, distilled water. A 4 $\mu$L aliquot of each sample was then diluted to a final protein concentration of ≈0.1 mg/mL in 40 $\mu$L of a solution containing 1.5 mg/mL α-cyano-4-hydroxycinnamic acid in 25% aqueous methanol. These samples were then deposited as a series of 500 nL spots on top of an air-dried layer of matrix made by spotting 5 $\mu$L of a 30 mg/mL solution of α-cyano-4-hydroxycinnamic acid in pure methanol. Samples were subsequently air-dried before mass spectral analyses, performed in the mass spectrometer adjusted to reflectron mode settings suitable for low mass determination (500−2500 Da).

An identical experiment was carried out with $Zn_6$ MTF-zf bound to a 23-base pair oligonucleotide containing a single copy of the MREd sequence from the mouse MT-I promoter (*27*), formed anaerobically by mixing 2.0 mL of 5 $\mu$M $Zn_6$ MTF-zf with 28 $\mu$L of a 730 $\mu$M MREd solution for 15 min (10 $\mu$M MREd), prior to addition of $d_5$-NEM as described above. The samples were processed in exactly the same way as free MTF-zf samples. For the experiments that probed the reactivity of Cys thiolates in $Zn_5$ MTF-zf26, 12 $\mu$L 0.10 M $d_5$-NEM was added to 2.0 mL 4.76 $\mu$M $Zn_5$ MTF-zf26 (0.60 mM $d_5$-NEM final; 12.6-fold excess over cysteine thiolates). At some pulse time, *t*, 200 $\mu$L was withdrawn and added to a solution containing 80 $\mu$L 0.5 M NaCl and 24 $\mu$L 0.1 M $H_5$-NEM, for a final concentration of 7.89 mM $H_5$-NEM (13.2:1.0 $H_5$-NEM:$d_5$-NEM). This sample was then divided into two parts, and 10 $\mu$L of 0.1 mg/mL solution of trypsin or 0.125 mg/mL chymotrypsin added to each tube. The digestion reactions were allowed to proceed for at least 3 h at ambient temperature, and the resulting peptides prepared for mass spectrometry essentially as described above. For the $Zn_5$ MTF-zf26:MREd complex, an identical experiment was carried out except that 8.76 $\mu$M MREd oligonucleotide was present in the pulse-chase.

To measure the reactivity rate profiles of cysteine thiolate pairs in Sp1-zf, 10 $\mu$L of 0.10 M $d_5$-NEM was added at time zero to 600 $\mu$L of 25 $\mu$M $Zn_3$ Sp1-zf (150 $\mu$M Cys residues; 1.64 mM $d_5$-NEM), incubated for various lengths of time, whereupon 50 $\mu$L aliquots were withdrawn and mixed with a solution containing with 10 $\mu$L of 0.10 M $H_5$-NEM, 80 $\mu$L of 0.5 M NaCl, and 2 $\mu$L of 1 mg/mL sequence grade trypsin (12.1:1.0 $H_5$-NEM:$d_5$-NEM). These samples were allowed to digest in the glovebox overnight. One-tenth of each sample (6 $\mu$L) was then diluted to a final protein concentration of ≈0.1 mg/mL in 2 $\mu$L of a 1.5 mg/mL ferulic acid in 25% aqueous methanol. These samples were then deposited as a series of 500 nL spots on top of an air-dried layer of matrix made by spotting 5 $\mu$L of a 30 mg/mL solution of α-cyano-4-hydroxycinnamic acid in pure methanol. Control experiments were also carried out with apo Sp1-zf, generated by incubating $Zn_3$ Sp1-zf with 300 $\mu$M EDTA, or in the presence of 2 mol equivalents of excess Zn(II). Sp1-zf samples were subjected to mass spectrometry exactly as described above. In all cases, two independent pulsed alkylation/mass spectrometry experiments were carried out for each sample condition, one of which was used to collect data at shorter times (0−60 min $d_5$-NEM pulse) and one at long times (40−250 min) with the combined data simultaneously analyzed as described below.

*MALDI-TOF Mass Spectrometry*. MALDI-TOF mass spectra of all samples were acquired using a Perseptive Biosystem Voyager Elite XL TOF mass spectrometer equipped with a pulsed nitrogen laser emitting at 337 nm manufactured by Laser Science Inc. All spectra were acquired in the positive ion mode using 25 kV acceleration. Each spectrum is the average of 100 laser pulses. The spectra for the tryptic and chymotryptic peptides of MTF-zf were acquired with 200 ns delayed extraction in reflectron mode. The grid and the guide wire voltages were operated at 70 and 0.05% of the acceleration voltage, respectively. Bradykinin $[1060.5\ Da]^{1+}$ was used as external calibration for the mass spectrometer prior to mass analyses of tryptic and chymotryptic peptides. The mass resolution achieved with this experiment is routinely 0.2 ppm, with typically reproducibility between samples of ± 0.2 ppm.

A single MALDI-TOF mass spectrum was acquired for each $d_5$-NEM time pulse-$H_5$-NEM chase experiment and processed using GRAMS 32 for peak localization and integration. Each mass spectrum contains a complete set of tryptic (or chymotryptic) peptides except that all cysteine-containing peptides are fully alkylated at each of the two cysteine residues by NEM, which are resolved as either $H_5$,$H_5$-NEM derivatized peptides (mass = expected peptide mass + 250 mu), $d_5$,$H_5$-NEM derivatized peptides (mass = expected peptide mass + 255 mu), or as $d_5$,$d_5$-NEM derivatized peptides (mass = expected peptide mass + 260 mu) by mass spectrometry (Figure 2). The sequences of the tryptic and chymotryptic peptides used for this purpose are listed in Table 1. The mol fraction (Θ) of each of the three doubly derivatized peptides in a mixture is simply given as the ratio of the peak area integration (A) of the *i*th NEM-derivatized species to the sum of the integrated areas of all ($H_5$,$H_5$ + $H_5$,$d_5$ + $d_5$,$d_5$) alkylated species. For example, the mol fraction of the $d_5$,$d_5$-derivatized peptide, $\Theta(d_5,d_5)$, is defined as

$$\Theta(d_5,d_5) = A(d_5,d_5)/[A(H_5,H_5) + A(H_5,d_5) + A(d_5,d_5)]$$

As the pulse time of $d_5$-NEM reactivity increases, $\Theta(d_5,d_5)$ will increase with other species correspondingly decreasing. Any cysteine thiolate that survives the $d_5$-NEM pulse is then fully alkylated in the chase by an NEM solution containing ≈10:1 molar ratio of $H_5$-NEM to $d_5$-NEM. A chase designed in this way will derivatize all unmodified two-Cys containing peptides that survive the $d_5$-NEM with an isotopic distribution of $H_5$,$H_5$:$H_5$,$d_5$:$d_5$,$d_5$ of ≈10:1:0.1. Thus, the mole fraction of reactive zinc finger cysteine pairs for the *j*th zinc finger domain peptide ($ZF_j$) which are alkylated in the $d_5$-NEM pulse, Θ(reactive $ZF_j$), will not be substantially perturbed by this chase composition. Therefore,

$$\Theta(\text{reacted } ZF_j) = \Theta(d_5,d_5)$$

The mole fraction of unmodified zinc finger domain peptides,

Table 1: Amino Acid Sequences and Masses of NEM-Labeled Zinc Finger Peptides Used in the Ratiometric Pulsed Alkylation/Mass Spectrometry Experiments

| zinc finger | amino acid sequence of MTF-1 zinc finger peptides | mass of the peptide (Da)[a] | mass of NEM-labeled peptides (Da) | | | | | |
|---|---|---|---|---|---|---|---|---|
| | | | $H_5$, $H_5$ | | $H_5$, $d_5$ | | $d_5$, $d_5$ | |
| | | | observed | calculated | observed | calculated | observed | calculated |
| F1 | $^{140}$YQ**C**TFEG**C**PR | 1203.49[T] | 1453.05 | 1453.58 | 1458.08 | 1458.14 | 1463.11 | 1463.17 |
| F2[b] | $^{169}$TFV**C**NQEG**C**GKAF (MTF-zf) | 1403.60[C] | 1653.55 | 1653.70 | 1658.55 | 1658.25 | 1663.59 | 1663.28 |
| F2[b] | $^{171}$V**C**NQEG**C**GKAF (MTF-zf26) | 1155.49[C] | 1405.50 | 1405.58 | 1410.50 | 1410.14 | 1415.20 | 1415.17 |
| F3 | $^{197}$EKPFE**C**DVQG**C**EK | 1511.65[T] | 1761.10 | 1761.74 | 1766.15 | 1766.30 | 1771.29 | 1771.33 |
| F4 | $^{230}$R**C**DHDG**C**GKAF | 1208.49[C] | 1458.45 | 1458.58 | 1463.47 | 1463.14 | 1468.52 | 1468.17 |
| F5 | $^{260}$R**C**DHDG**C**GKAF | 1208.49[C] | 1458.45 | 1458.58 | 1463.47 | 1463.14 | 1468.52 | 1468.17 |
| F6 | $^{282}$THTRGERPFF**C**PSNG**C**EK | 1909.83[T] | 2159.15 | 2159.92 | 2164.17 | 2164.48 | 2169.21 | 2169.51 |

| zinc finger | amino acid sequence of Sp1 zinc finger peptides | mass of the peptide (Da) | mass of NEM-labeled peptides (Da) | | | | | |
|---|---|---|---|---|---|---|---|---|
| | | | $H_5$, $H_5$ | | $H_5$, $d_5$ | | $d_5$, $d_5$ | |
| | | | observed | calculated | observed | calculated | observed | calculated |
| F1 | $^{625}$QHI**C**HIQGCGK | 1223.58[T] | 1473.88 | 1473.67 | | 1478.23 | 1483.82 | 1483.26 |
| F2 | $^{649}$WHTGERPFM**C**TWSY**C**GK | 2088.89[T] | 2338.88 | 2338.98 | | 2343.54 | 2348.58 | 2348.57 |
| F3 | $^{686}$FA**C**PE**C**PK | 894.39[T] | 1144.92 | 1144.48 | | 1149.04 | 1154.98 | 1155.07 |

[a] T, peptide generated by tryptic digestion; C, peptide generated by chymotryptic digestion. [b] Zinc finger F2 peptide in MTF-zf failed to yield appreciable chymotryptic cleavage following Phe170, unlike MTF-zf26.

$\Theta$(unmodified $ZF_j$) is therefore given by

$$\Theta(\text{unmodified } ZF_j) = \Theta(H_5,d_5) + \Theta(H_5,H_5) = 1 - \Theta(d_5,d_5)$$

For the Sp1-zf experiments, $\Theta(H_5,d_5)$ comprised less than 5% of the total species (expected value is ≈7% from the chase composition), which was near the limit of detection in these mass spectrometry runs. In contrast, all experiments carried out with MTF-zf (± MRE) contained ≈15−20% $H_5$,$d_5$-peptides at all zinc finger sites at the earliest pulse time points (expected value is 10%). Since the pseudo-first-order rate of decay of the $H_5$,$d_5$-peptides was essentially identical to that measured for the $H_5$,$H_5$-peptides and build-up of the $d_5$,$d_5$-peptides (see Results), we attribute these mixed alkylated species as deriving from uncertainties in the $H_5$-NEM:$d_5$-NEM ratio in the chase solution, rather than partially reactive species formed during the $d_5$-NEM pulse. For the MTF-zf26 experiments, $\Theta(H_5,d_5)$ comprised 8−12% of the total species (expected value is ≈8%) and did not decay in a measurable way during the course of the reaction. Except where indicated, all plots of $\Theta$(unmodified $ZF_j$) were satisfactorily fit to a first-order exponential decay, as expected. Note that since this is a ratiometric experiment which quantifies the *relative* quantities of isotopically differentiated peptides, the quantitation is not complicated by problems associated with *absolute* intensity mass spectral analysis, which include sample heterogeneity, shot-to-shot variability, and sample-to-sample inconsistencies in ion abundance due, for example, to incomplete protease digestion with the proteases.

*Fluorescence Anisotropy Experiments.* The change in the steady-state anisotropy of coumarin-labeled MREd duplex upon addition of MTF-zf or MTF-zf26 was measured in the L-format (40 mM Mops, pH 7.0, 0.20 M NaCl, 25 °C) exactly as described previously (*22*, *27*).

## RESULTS

*Cysteine Thiolate Alkylation Profiles with the Model Zinc Finger Protein, Sp1-zf.* A stack plot of representative sections of MALDI-TOF mass spectra derived from different $d_5$-NEM pulse times selected to show the isotopic distribution of the doubly-NEM derivatized tryptic peptides which correspond to zinc finger F2 (Table 1) of $Zn_3$ Sp1-zf is shown in Figure 3A. Analogous sections selected to show reactivity profiles for F1 and F3 are not shown due to space considerations. Note that $H_5$,$H_5$-, $d_5$,$H_5$-, and $d_5$,$d_5$-NEM derivatized peptides are cleanly separated in the mass spectrum in a manner consistent with their expected isotopic distributions, with sufficient signal-to-noise for quantitation of individual peptide species. Second, as expected, as the pulse time with $d_5$-NEM increases, there is a greater fraction of doubly alkylated F2 peptide containing two $d_5$,$d_5$-NEM adducts, with a corresponding decrease in the fraction of peptides recovered as $H_5$,$H_5$-derivatized peptides (not shown). In no case, under these conditions, does the mixed derivatized $H_5$,$d_5$-peptide accumulate to appreciable fraction of the total alkylated species. Since under all conditions, NEM is in great molar excess over cysteine thiolates, the rates of decay of $H_5$,$H_5$-peptide and appearance of $d_5$,$d_5$-peptide each follow a pseudo-first-order process (Figure 3C) characterized by a rate constant of reactivity, $k_{app}$, of 5.4 (± 0.3) × $10^{-3}$ $min^{-1}$. If $k_{app}$ is expressed as a function of the total $d_5$,$d_5$-NEM concentration (1.64 mM), an apparent second-order rate constant of 3.26 (± 0.23) $M_{NEM}^{-1}$ $min^{-1}$ is obtained (Table 2).

Figure 3B shows that coordination to Zn(II) by F2 results in a substantial protection against cysteine thiolate reactivity as expected (*30*), since all cysteine thiolates are fully derivatized during the $d_5$-NEM pulse time when the reaction is run in the presence of excess EDTA. Although the rate of reaction of Zn(II)-free thiolates was too fast to measure from this experiment, a lower limit for the apparent second-order rate constant is >5000 $M_{NEM}^{-1}$ $min^{-1}$, or greater than 250 times faster than in the presence of Zn(II). This rate constant is of the same order of magnitude as the true second-order rate constant measured for the alkylation of the sulfhydryl group of glutathione ($k$ = 38 000 $M_{NEM}^{-1}$ $min^{-1}$) (*41*) and faster than the solvent-exposed Cys106 in the α-subunit of bacterial luciferase ($k$ = 1670 $M_{NEM}^{-1}$ $min^{-1}$) under similar

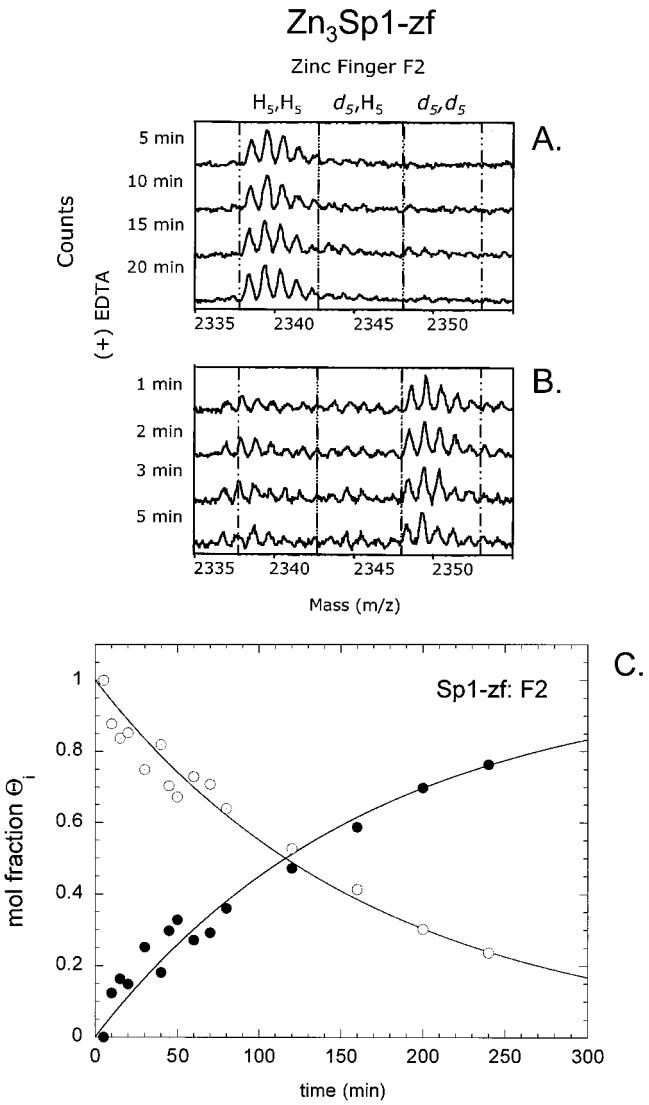


FIGURE 3: Selected regions of the pulsed-alkylation MALDI-TOF mass spectra for trypsin-digested $Zn_3$ Sp1-zf (A), and $Zn_3$ Sp1-zf treated with excess EDTA (B) acquired as function of the $d_5$-NEM pulse time indicated on the left-hand side of the figure. The mass spectral regions are shown for the $H_5$,$H_5$-, $d_5$,$H_5$-, and $d_5$,$d_5$-derivatized F2 tryptic peptides of Sp1-zf. (C) Plot of the mol fraction of the $H_5$,$H_5$-F2 (⊙) and $d_5$,$d_5$-F2 (●) peptide as a function of $d_5$-NEM pulse time. The solid line through the experimental data is a least-squares fit to a first-order reaction (see Materials and Methods) defined by the rate constant, $k_{app} = 5.4\ (\pm\ 0.3) \times 10^{-3}\ min^{-1}$.

solution conditions (pH = 7.0, 25 °C) (*42*). The kinetics of pulsed alkylation of the F1 thiolates in $Zn_3$ Sp1 are indistinguishable from that of the F2 cysteine pair, with $k_{app} = 5.3\ (\pm\ 0.3) \times 10^{-3}\ min^{-1}$ (Table 2). In contrast to F1 and F2, the alkylation profile for F3 thiolates in $Zn_3$ Sp1-zf is best described by a sum of two exponentials of approximately equal amplitude, with the second slower phase ($A_s = 0.54$) indistinguishable from that of F1 and F2, with $k_{app} = 4.9\ (\pm\ 1.2) \times 10^{-3}\ min^{-1}$ (Table 2). The faster phase ($A_f = 0.46$) is ≈21-fold faster, with $k_{app} = 0.11\ (\pm\ 0.03)\ min^{-1}$. Repeating this experiment in excess Zn(II) has no effect (data not shown). The structural origin for the two distinct phases of pulsed alkylation for F3 thiolates is unknown but may be reporting on two (or more) distinct conformations of F3 in $Zn_3$ Sp1-zf which coexist in solution. F3 of Sp1-zf differs from F1 and F2 in that it is characterized by Cys−***X₂***−Cys (Cys−Pro−Glu−Cys−Pro) sequence, while F1 and F2 have Cys−***X₄***−Cys sequences (*43*).

Table 2: Apparent Second Order Rates of Reactivity of Cysteine Pairs ($k_{app}$) in Individual Zinc Fingers in MTF-zf, MTF-zf26, and Sp1-zf in the Presence and Absence of Bound DNA[a]

| protein | $k_{app}$ ($M_{NEM}^{-1}\ min^{-1}$) | | fold-protection[b] |
|---|---|---|---|
| MTF-zf: | −MREd | +MREd | |
| F1 | 5.66 (± 0.35) | 0.30 (± 0.01) | 18.9 |
| F2 | 1.42 (± 0.55) | 0.34 (± 0.16) | 4.2 |
| F3 | 3.80 (± 0.40) | 0.72 (± 0.14) | 5.3 |
| F4 | 2.50 (± 0.33) | 0.71 (± 0.21) | 3.5 |
| F5 | 43.8 (± 3.3) | 1.40 (± 0.21) | 31.3 |
| F6 | 23.0 (± 5.5) | 2.51 (± 0.37) | 9.2 |
| MTF-zf26: | | | |
| F2 | 2.02 (± 0.14) | 0.92 (± 0.14) | 2.2 |
| F3 | 3.39 (± 0.23) | 1.61 (± 0.10) | 2.1 |
| F4 | 12.8 (± 0.4) | 5.94 (± 0.18) | 2.2 |
| F5 | 22.3 (± 1.2) | 13.1 (± 0.9) | 1.7 |
| F6 | 24.7 (± 1.8) | 15.0 (± 0.8) | 1.6 |
| Sp1-zf: | | | |
| F1 | 3.25 (± 0.20) | N.D.[c] | N.D.[c] |
| F2 | 3.26 (± 0.23) | N.D.[c] | N.D.[c] |
| F3 | 2.99 (± 0.74) ($A_s = 0.54$)[d] | N.D.[c] | N.D.[c] |
| | 67.1 (± 18.3) ($A_f = 0.46$) | | |

[a] Determined as described in Materials and Methods (see Figures 4, 5, and 7). [b] $k_{app}^{-MREd}/k_{app}^{+MREd}$. [c] Not determined. [d] Two rate constants were resolved from these data (see text for details).

These control experiments with Zn(II)-saturated Sp1-zf show that the reactivity profiles of cysteine thiolate pairs within the three-finger domain fragment are nearly identical and follow the expected pseudo-first-order kinetics of alkylation, at least with F1 and F2 thiolates. Furthermore, the data suggest that the distinct characteristic of F3 that leads to two resolvable kinetic phases has no effect on the neighboring zinc finger domain F2, since the reactivity profile of F1 is indistinguishable from that of F2. This result suggests that the intrinsic reactivities of individual zinc finger domains may not be strongly influenced by alkylation at neighboring finger domains. This is the expected behavior of three independently folded, noninteracting zinc finger domains that are connected by flexible tethers, which likely characterizes uncomplexed Sp1-zf well (*43*, *44*).

*Cysteine Thiolate Reactivities in Individual Zinc Fingers in the Uncomplexed and the MREd-Bound Forms of $Zn_6$ MTF-zf.* The mass spectral peaks used for the quantitation of the $d_5$,$d_5$-, $H_5$,$d_5$-, and $H_5$,$H_5$-alkylated peptides for each of the zinc finger cysteine pairs of MTF-zf are given in Table 1. Note the excellent agreement between expected and observed masses (in most cases within 5 ppm). Figure 4 shows a superposition of two independent experiments, with selected regions of individual mass spectra shown for the chymotryptic zinc finger peptides corresponding to zinc fingers F2 and F5, in the presence and absence of bound MREd oligonucleotide. From simple inspection of these data, it is clear that the alkylation rate constant of F5 thiolates is greater than the F2 thiolates in the absence of the MREd. However, when bound to the MREd, *both* cysteine pairs are strongly protected from alkylation (see below). For each finger fragment, the peak intensities were quantitated, and the mole fraction of each species ($\Theta_i$) was determined as described under Materials and Methods. Representative plots of the data obtained for F1 and F6 thiolate pairs are shown

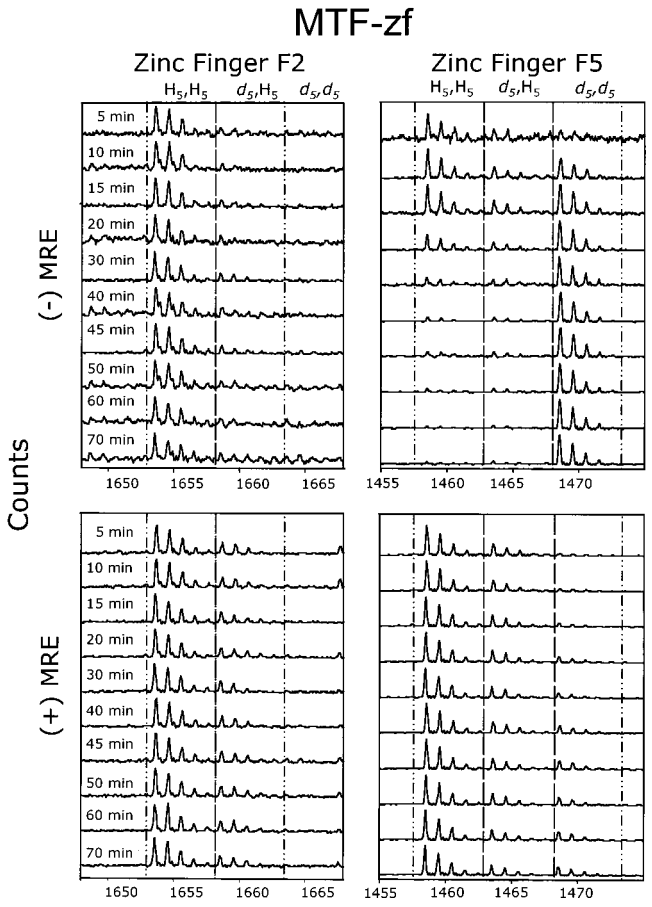


FIGURE 4: Selected regions of the pulsed-alkylation MALDI-TOF mass spectra for chymotrypsin-digested $Zn_6$ MTF-zf in the absence (upper two panels) and presence (lower two panels) of a 2-fold molar excess of 23-base pair MREd oligonucleotide acquired as function of the $d_5$-NEM pulse time indicated. The mass spectral regions for the $H_5$,$H_5$-, $d_5$,$H_5$- and $d_5$,$d_5$-derivatived F2 (left) and F5 (right) chymotryptic peptides are shown.

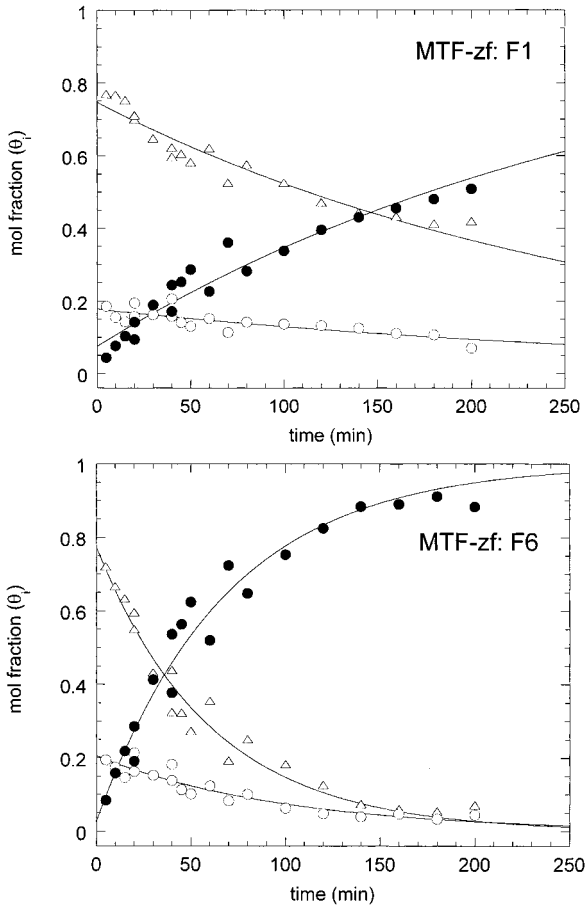


FIGURE 5: Plot of the mole fraction of the $H_5$,$H_5$- (Δ), $d_5$,$H_5$- (○), and $d_5$,$d_5$- (●) derivatived MTF-zf F1 (A) and MTF-zf F6 (B) tryptic peptides obtained as a function of $d_5$-NEM pulse time. The solid line through the experimental data is a least-squares fit to a first-order reaction (see Materials and Methods) defined by the following rate constants and amplitudes: For MTF-zf F1, the disappearance of the $H_5$,$H_5$ peptide is defined by the parameters $k_{app} = 3.6 (\pm 0.3) \times 10^{-3}$ min$^{-1}$, $\Theta_0 = 0.75$; for the $d_5$,$H_5$ peptide, $k_{app} = 3.2 (\pm 0.1) \times 10^{-3}$ min$^{-1}$, $\Theta_0 = 0.18$. The appearance of $d_5$,$d_5$-F1 peptide is defined by $k_{app} = 3.5 (\pm 0.2) \times 10^{-3}$ min$^{-1}$, $\Theta_0 = 0.07$. The average rate constant from these three determinations is $k_{app} = 3.4 (\pm 0.3) \times 10^{-3}$ min$^{-1}$. For MTF-zf F6, the disappearance of the $H_5$,$H_5$ peptide is defined by the parameters $k_{app} = 1.66 (\pm 0.12) \times 10^{-2}$ min$^{-1}$, $\Theta_0 = 0.78$; for the $d_5$,$H_5$ peptide, $k_{app} = 1.02 (\pm 0.13) \times 10^{-2}$ min$^{-1}$, $\Theta_0 = 0.21$. The appearance of $d_5$,$d_5$-F1 peptide is defined by $k_{app} = 1.47 (\pm 0.11) \times 10^{-2}$ min$^{-1}$, $\Theta_0 = 0.25$. The average rate constant from these three determinations is $k_{app} = 1.38 (\pm 0.33) \times 10^{-2}$ min$^{-1}$.

in Figure 5 in the absence of DNA. As can be seen, F6 thiolates are considerably more reactive than are F1 thiolates, with an apparent second-order rate constant of 5.7 (± 0.4) $M_{NEM}^{-1}$ min$^{-1}$ for F1 cysteines versus 23.0 (± 5.5) $M_{NEM}^{-1}$ min$^{-1}$ for F6 thiolates, or approximately 5-fold faster under these conditions (Table 2). For comparison, the same analysis for F3 thiolates gives $k_{app} = 3.8$ (± 0.4) $M_{NEM}^{-1}$ min$^{-1}$ or about 8-fold slower that F6 cysteines.

Figure 6A shows a bar plot of the apparent second-order rate constants obtained for the kinetics of the appearance of the fully derivatized $d_5$,$d_5$-peptide for all of the finger domain cysteine pairs in MTF-zf in the presence and absence of bound MREd oligonucleotide. These data are also summarized in Table 2. In contrast to Sp1-zf, the rate constants for pulsed alkylation are remarkably nonuniform. The data suggest that uncomplexed $Zn_6$ MTF-zf contains roughly two classes of reactive Cys pairs, with F5 and F6 thiolates far more reactive than the N-terminal four finger domains. Interestingly, the metal complex formed by F1 appears to be slightly more kinetically labile than the F2, F3, and F4 complexes, but only by a factor of ≈2; this reaction rate is also within a factor of ≈2 of that measured for the Sp1 zinc finger domains. These results are consistent with previous findings that identified at least two classes of zinc sites in MTF-zf based on their apparent affinities for Zn(II) (*22*, *27*), with 2−3 zinc sites of relatively lower affinity and 3−4 of high affinity. These pulsed alkylation experiments provide direct evidence that F5 and F6 are indeed the weak zinc-binding fingers of MTF-zf (*27*), with finger domains F1−F4 forming very stable complexes with the metal.

The reactivities of all finger domains in MTF-zf are strongly reduced when bound to the high affinity MREd oligonucleotide, with F6 becoming the most reactive finger domain in the protein−DNA complex (Figure 6A; Table 2). These findings are consistent with previous near UV−CD studies that showed each of the zinc fingers in MTF-zf makes a detectable contribution to the structural changes induced into the MREd upon binding as well as to the overall binding affinity (*27*). Clearly, however, fingers F1−F4 make the greatest contribution to DNA complex stability (*27*).

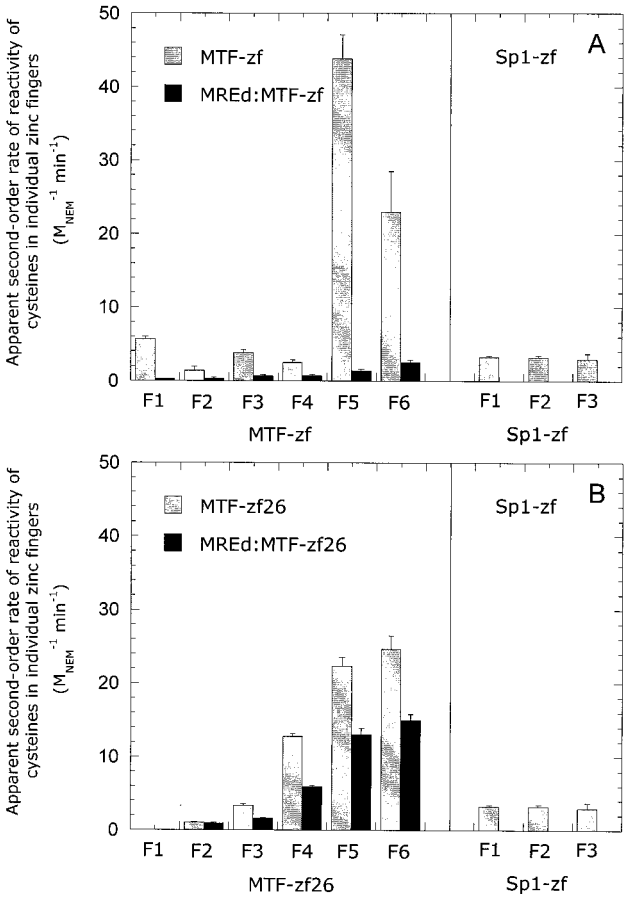


FIGURE 6: (A) Bar chart representation of the average apparent second-order rate constants measured for alkylation of cysteine pairs in each of the six zinc fingers for $Zn_6$ MTF-zf (left side of figure) and for $Zn_3$ Sp1-zf (right side of figure, gray bars), the former in the absence (gray bars) and presence (black bars) of bound MREd oligonucleotide. (B) Bar chart plot of the apparent second-order rate constants measured for alkylation of cysteine pairs in each of the five zinc fingers for $Zn_5$ MTF-zf26 in the absence (gray bars) and presence (black bars) of a 2-fold excess of MREd oligonucleotide. The same data are shown for $Zn_3$ Sp1-zf on the right side of the figure for comparison.

*Cysteine Thiolate Reactivities in Individual Zinc Fingers in the Uncomplexed and the MREd-Bound Forms of $Zn_5$ MTF-zf26, a ΔF1 Deletion Mutant.* A recently proposed functional model of MTF-1 activity invokes a special role for zinc finger F1 in reversible activation of high affinity MRE binding by low affinity Zn(II) binding to this zinc finger domain (*28*). This model makes the prediction that F1 would have a lower affinity for Zn(II) than the other finger domains. Furthermore, functional characterization of ΔF1 MTF-1 in vivo suggested that this form of intact MTF-1 is a constitutive activator of MRE-driven reporter gene expression, a finding that makes the prediction that ΔF1 MTF-zf would have high affinity for the MREd, whose binding activity could not be modulated by exogenous Zn(II). It was therefore of interest to characterize $Zn_5$ MTF-zf26 in our pulsed alkylation experiments.

The apparent second-order rates of reactivity presented in a bar chart format are shown in Figure 6B, which enables a direct comparison with $Zn_6$ MTF-zf (Figure 6A) carried out under exactly the same conditions (see also Table 2). These data show that, as with MTF-zf, F2 and F3 are the slowest reacting finger domains in the molecule. In striking contrast,

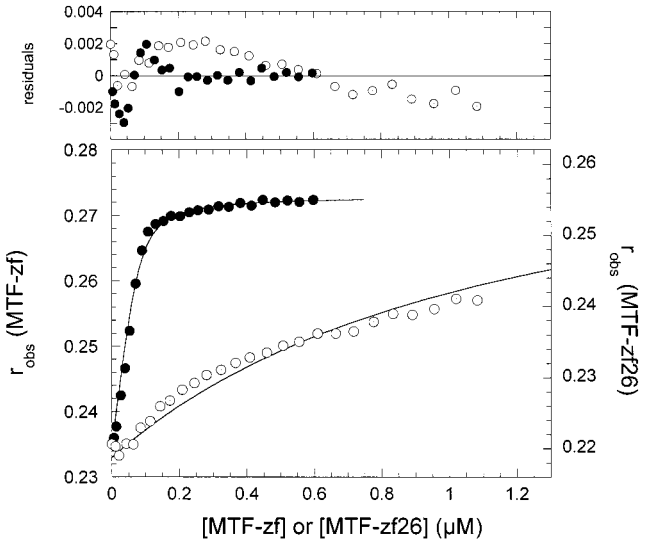


FIGURE 7: Binding isotherms of $Zn_6$ MTF-zf (●) and $Zn_5$ MTF-zf26 (⊙) to a coumarin-labeled 23-base pair MREd-containing oligonucleotide duplex of the same sequence as used panel A (81 nM duplex, 40 mM Mops, 0.20 M NaCl, pH 7.0, 25 °C). The solid curve in each case defines a fit to a 1:1 binding model. For MTF-zf, $K_a = 1.05 (\pm 0.17) \times 10^8$ $M^{-1}$; $r_{max} = 0.273$. For MTF-zf26, $K_a = 1.03 (\pm 0.15) \times 10^6$ $M^{-1}$; $r_{max}$ fixed at 0.268 (or comparable to the change in $r$ with MTF-zf. The residuals are shown in the top portion of the figure. MTF-zf (●); MTF-zf26 (⊙).

the F4 domain thiolates in MTF-zf26 are highly reactive toward $d_5$-NEM, with $k_{app}$ within a factor of 2 of the cysteine pairs in the C-terminal finger domains F5 and F6. Furthermore, the protection afforded by MREd binding is far less than that observed for cysteines in the MTF-zf-MRE complex and is never larger than a factor of approximately two (Figure 6B; Table 2), a result that suggests a significantly lower equilibrium binding affinity for the MREd. Consistent with this, a fluorescence anisotropy-based DNA binding experiment reveals that $Zn_5$ MTF-zf26 binds to a coumarin-labeled MREd oligonucleotide ≈100-fold more weakly than MTF-zf (Figure 7). In fact, the binding isotherm for MTF-zf26 is not well modeled by a simple 1:1 binding model and may be indicative of essentially nonspecific binding or two of more MTF-zf26 monomers. Interestingly, the addition of 50 μM Zn(II) to these binding assays increases the apparent affinity of MTF-zf26 for the MREd sequence by a factor of approximately 10 (data not shown). We conclude that deletion of F1 from MTF-zf is markedly destabilizing, both toward the structure of the uncomplexed zinc finger domain and toward MTF-zf-MREd complex formation.

*Evidence against Independent Reactivity of Cysteines in Internal Zinc Fingers in MTF-zf.* If all the zinc fingers of MTF-zf behave in solution as independent folded domains connected by flexible tethers, the kinetics of reaction at each thiolate pair should obey pseudo-first-order kinetics under these conditions. A more detailed analysis of the kinetics of alkylation of cysteine thiolates in MTF-zf F4, in particular (Figure 8A), reveals that these progress curves are modeled better by a sequential two-step mechanism

$$A \rightarrow B \rightarrow C$$

defined by the rate constants $k_1^{app}$ and $k_2^{app}$, with C corresponding to the doubly alkylated F4 peptide. If the value of one of these rate constants is constrained to $k_{app}$ for the

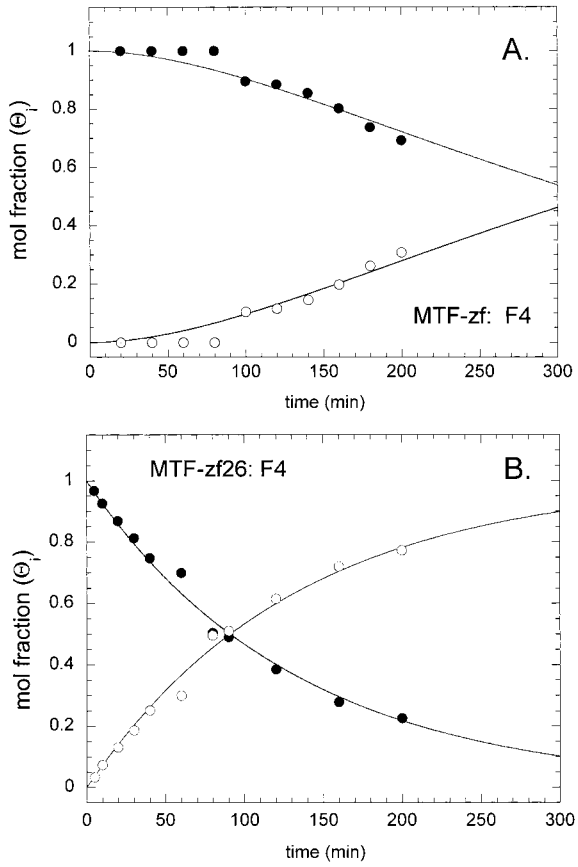


FIGURE 8: Plot of the mol fraction of the $H_5$,$H_5$- (●) and $d_5$,$d_5$- (⊙) derivatize MTF-zf F4 (A) and MTF-zf26 F4 (B) tryptic peptide as a function of $d_5$-NEM pulse time. For MTF-zf F4, the solid line through each set of experimental data is a least-squares fit to two-step sequential model (see text for details), in which $k^1_{app}$ was constrained to the value for $k_{app}$ for MTF-zf F1 thiolates or $5.24 \times 10^{-3}$ min$^{-1}$, with $k^2_{app}$ optimized to be 5.14 ($\pm$ 0.44) $\times 10^{-3}$ min$^{-1}$. For the MTF-zf26 F4 peptide, the solid line is a least-squares fit to a first-order reaction defined by the rate constant, $k_{app} = 7.6$ ($\pm$ 0.2) $\times 10^{-3}$ min$^{-1}$.

alkylation of F1 cysteines ($k_{app} = 5.2 \times 10^{-3}$ min$^{-1}$), the optimized value for the other is 5.1 ($\pm$ 0.4) $\times 10^{-3}$ min$^{-1}$. Thus, the reactivity profile of F4 thiolates (and to a lesser extent F3 thiolates; data not shown) may well be dependent in some way on the prior alkylation of F1 cysteine pairs; however, this conclusion must be viewed with caution since these rate constants obviously do not represent a unique fit to the data. Regardless of the molecular explanation, this situation contrasts sharply with that obtained for a ΔF1 finger deletion of MTF-zf, MTF-zf26 (Figure 8B). Here, the derivatization of F4 thiolates clearly follows pseudo-first-order kinetics and, as mentioned above, these cysteines are highly reactive (see Discussion).

## DISCUSSION

In this paper, we present a new application of ratiometric pulsed alkylation mass spectrometry (*38*) to probe the residue-specific kinetics of reaction of cysteines in zinc finger proteins with a sulfhydryl-specific alkylating reagent, *N*-ethylmaleimide. Although NEM will potentially react with other nucleophiles, we could find no evidence for derivatization of other amino acid residues under these solution conditions, with fully alkylated MTF-zf or Sp1-zf each characterized by a molecular mass consistent with the addition of 12 and 6 NEM groups per peptide chain, respectively. The method we outline here is perfectly general, i.e., any residue-specific reagent that results in a satisfactory increase in the molecular mass of the protein can be used and, when carried out in a ratiometric mode is particularly powerful, since the quantitation of the kinetics of reactivity relies only the *relative*, rather than *absolute*, amounts of deuterated and protiated peptides resolved by the mass spectrometer. This mass spectrometry-based method is exactly analogous to previously described radioisotope-based ratiometric [$^3$H]/[$^{14}$C] acetylation used to probe the intrinsic reactivities of lysine residues toward [$^3$H]- vs [$^{14}$C]-acetic anhydride (*45*).

*General Considerations of the Application of the Technique to Zinc Finger Proteins.* Canonical $Cys_2-His_2$ zinc finger domains are ≈30-amino acid $\beta\beta\alpha$ structural motifs that coordinate a Zn(II) ion through the conserved Cys and His side chains (*47*). The two Cys residues are derived from a short two-stranded antiparallel $\beta$-sheet, with the two His side chains derived from the immediately following α-helix. The binding of Zn(II) induces the folding of the $\beta\beta\alpha$ structure (*47*), which is further stabilized by a mini-hydrophobic core packed on top of the zinc chelate in the junction region between the $\beta\beta$- and α-structural domains (*48*). In solution structural studies of the zinc finger proteins that contain multiple, tandemly linked $\beta\beta\alpha$ zinc finger domains, e.g., the N-terminal three domains of TFIIIA (*44*), there is little evidence for any physical association between finger domains in the absence of DNA. In this case, the intrinsic reactivities of individual cysteine residues within a multifinger protein will be governed largely by two (local) factors: the solvent accessibility of the $S^\gamma$ atoms and the kinetic stability (or liability) of the Zn(II)-$S^\gamma$ coordination bonds within a particular zinc finger domain. Inspection of the solution structures of isolated zinc finger domains from a variety of proteins suggests that although there may be small differences in local structure, the overall architecture of the domain is essentially constant. Thus, intrinsic reactivity of Cys thiolates in zinc finger domains may well be largely determined by the stability of Zn(II)-$S^\gamma$ coordination bonds, particularly if one makes the further simplifying assumption that an $S^\gamma$ atom tied up in a metal coordination bond is a far poorer nucleophile toward electrophilic attack by NEM relative to the transiently formed unliganded thiolate group (*30*). In this simplest case, the relative rates of alkylation become a direct reporter on the dissociation equilibrium of an individual Zn(II)-$S^\gamma$ coordination bond. Although this was not rigorously established in these studies, we have shown that Zn(II) binding to liganding cysteine thiolates reduces the alkylation rate constant in the model zinc finger protein Sp1-zf by ≥ 1000-fold. It is important to point out, however, that if zinc finger domains interact strongly with one another, or the local electrostatic screening effects among isolated zinc finger domains are significantly different (*49*), then the rates of pulsed alkylation by NEM will be a more complex function of all of these factors.

Although the solution structure of free intact Sp1-zf has not yet been reported, there is no evidence to suggest that individual finger domains interact appreciably with one another when not bound to DNA, particularly with respect to F2 and F3 (*43*). Consistent with this, the slow rates of alkylation of individual cysteine pairs in $Zn_3$ Sp1-zf are

remarkably uniform (Figure 6). Inspection of the average solution structures of the F2 and F3 finger peptides of Sp1-zf reveals that in both domains, the $S^{\gamma}$ atom of the second Cys in the Cys−$X_{2\ or\ 4}$−Cys sequence is largely exposed to solvent, while the most N-terminal Cys is largely buried (*43*). Interestingly, the $S^{\gamma}$ atom of the second Cys in the Cys−***X*****$_2$**−Cys in F3 appears somewhat more exposed to solvent relative to that in the Cys−***X*****$_4$**−Cys F2 domain; this of course depends to some degree on the nature and side chain conformations of residues on the surface of the domain. In any case, we see no evidence for the accumulation of the $d_5$,$H_5$-derivatized peptide over the time course (hours) of the experiment (Figure 5); this would be expected if the singly alkylated zinc finger domain was a stable intermediate that was slowly converted to the fully $d_5$,$d_5$-derivatized adduct. This suggests that once one of the cysteines in a zinc finger structure is alkylated by NEM, the other cysteine in the Cys−$X_{2\ or\ 4}$−Cys sequence becomes highly reactive, due presumably to metal dissociation, and is rapidly alkylated. This behavior contrasts with what was found previously with $Cys_3$−His retroviral-type nucleocapsid protein zinc finger domains, where a singly alkylated zinc finger peptide accumulated as in intermediate to a fully derivatized peptide (*37*).

*Structural Conclusions for the Zinc Finger Domain of MTF-1.* In contrast to that which was observed for Sp1-zf, the alkylation profiles for the each of the zinc finger domains in the zinc finger fragment of MTF-1 are remarkably nonuniform (Figures 4−6). The C-terminal fingers are far more reactive than the other N-terminal zinc finger domains of the fragment, the latter of which are characterized by alkylation rate constants quite similar to Sp1-zf. This finding is consistent with the idea that there is clear structural heterogeneity among the zinc fingers of MTF-zf, and that this heterogeneity can be detected at the level of Zn(II)-$S^{\gamma}$ coordination bonds. Cysteine thiolates in finger domains F5 and F6 are far more reactive, which suggests the stabilities of these zinc chelates may well be lower. These domains correspond to the two zinc domains from which bound Zn(II) can be lost upon extensive dialysis (*22*). One possible interpretation of these findings is that the F5 and F6 do not actually adopt stable folded $\beta\beta\alpha$-structures in the presence of saturating Zn(II) under these conditions. In fact, previous far-UV CD studies were interpreted to suggest that one or more of the C-terminal fingers adopts an alternative conformation under conditions of saturating Zn(II) (*27*). Heteronuclear NMR studies of a peptide fragment encompassing the C-terminal F4, F5, and F6 finger domains, MTF-zf46, show that F4 and F6 do indeed adopt $\beta\beta\alpha$- structures, with F6 characterized by a lower affinity as determined by in a zinc titration experiment with apo-MTF-zf46 (*50*). Furthermore, at saturating Zn(II), F5 apparently does *not* adopt a stable $\beta\beta\alpha$-structure but is instead in equilibrium with an alternative, as yet undefined, conformation (*50*). This might explain its enhanced reactivity relative to F6. Regardless of the structural details, these data suggest that the stability of F5 is even less than that of F6 with both domains far less stable than that of the N-terminal fingers; this would give rise to the observed strongly enhanced reactivities of F5 and F6 thiolates toward NEM.

More detailed inspection of the alkylation rate profiles of free $Zn_6$ MTF-zf reveals that the N-terminal finger F1 is characterized by a reactivity that is slightly enhanced relative to F2, F3, and F4. In contrast, under all conditions, F2 and F4 thiolates are extremely slow to react, with the kinetics of reactivity of F4 cysteines, in particular, better modeled by a sequential mechanism (Figure 8A). Characterization of ΔF1 MTF-zf26 suggests that the N-terminal F1 domain plays some role in mediating this protection of F4 thiolates since deletion of the F1 domain results in conversion of F4 thiolates to an alkylation profile that obeys pseudo-first-order kinetics (Figure 8B), but reflective of a zinc complex that is kinetically quite labile (Figure 6). Although the interpretation of this experiment must be viewed with caution, one scenario that would give rise to this behavior is one where nonadjacent fingers F1 and F4 interact directly with one another, or alternatively, the presence of the F1 domain in MTF-zf stabilizes an intramolecular interaction between F4 and adjacent zinc domains. Only upon disruption of the F1 domain by alkylation do the F4 domain thiolates become susceptible to alkylation. There is at least one example of a $Cys_2$−$His_2$ zinc finger protein, mouse GLI, where it has been shown that adjacent fingers (F1 and F2) pack against one another, at least in the GLI-DNA complex (*51*). More detailed structural studies are required to substantiate this proposal.

*The MTF-zf:MREd Complex.* Previous limited trypsinolysis experiments revealed that the N-terminal fingers of MTF-zf are bound to the MREd in way in which these finger domains are protected from proteolysis (*27*). In contrast, the C-terminal finger domains F5 and F6 (C-terminal to Arg260; see Figure 1) are readily digested to smaller fragments by trypsin. This suggested that finger domains F5 and F6 may not be as intimately associated with the MREd as the N-terminal fingers. On the other hand, near-UV CD, FRET, and fluorescence anisotropy experiments suggested that C-terminal fingers made a detectable contribution to the structural changes induced on MTF-zf binding to the MREd oligonucleotide, as well as the affinity and specificity of the protein−DNA complex, perhaps through sequence nonspecific interactions (*27*). Our pulsed alkylation experiments reveal that the reactivity of all finger domains, including F5 and F6, are strongly protected from alkylation in the high affinity MTF-zf:MREd complex. Strikingly, F5 thiolates go from the most reactive in the uncomplexed molecule to within a factor of ≤ 3 of F1−F4 cysteines (Table 2). On the other hand, F6 shows the lowest fold-protection upon MREd binding and is 5−10-fold more reactive than F1−F4 thiolates toward alkylation by NEM in the complex. These results are fully compatible with previous studies and strongly suggest that F5, and to a lesser extent, F6 zinc finger domains interact directly with the DNA. A recent proposal for structure of the MTF-zf:MREd complex places these finger domains downstream of the highly conserved 5′-TGCRCNC core sequence element, overlapping the flanking GC-rich subdomain of the high affinity mMREd (*25*).

Although the differences are small, the N-terminal finger domain F1 becomes the least reactive in the protein−MREd complex and is also characterized by the second largest fold-reduction in alkylation rate constant, of nearly ≈19-fold (Table 2). This suggests that F1 is intimately associated with the DNA and may play a key role, directly or indirectly, in organizing the MTF-zf on the MREd in such a way that high affinity binding results. Consistent with this idea is the

finding that the ΔF1 MTF-zf26 binds quite weakly to the MREd, as measured directly by fluorescence anisotropy binding experiments (Figure 7) and the extent of protection of the cysteine thiolates from alkylation by NEM in the protein−DNA complex (Figure 6B; Table 2). Thus, F1 appears to play a critical role in stabilizing the overall structure of zinc finger fragment of the MTF-1, as well as in MTF-zf:MREd complex formation, either directly or indirectly. Recent studies of "finger-swap" mutants of Sp1-zf suggest that the C-terminal F3 zinc finger plays a primary role in maximizing the complementarity of the interactions between the nonadjacent F1 zinc finger and DNA major groove (*52*). A primary role of F1 in MRE-binding by MTF-1 is in contrast to a recent report that suggested that deletion of F1 from intact MTF-1 results in a protein that binds the MREd constitutively, at least as measured by gel mobility shift assays in crude cell extracts (*28*).

*Implications for the Mechanism of Metalloregulation by MTF-1.* Our findings establish that F5 and F6 zinc finger domains form less stable zinc chelates at equilibrium or are characterized by enhanced rates of microscopic dissociation of Zn(II)-$S^{\gamma}$ coordination bonds, relative to other domains of the molecule. If the mechanism of zinc-dependent activation of gene expression lies principally at the level of activation of DNA binding by reversible binding of Zn(II) to weak binding fingers of the molecule, these findings implicate zinc finger domains F5 and/or F6 as playing a functionally important roles in transcriptional activation in vivo. However, recent mammalian cell transfection experiments in which "missing-finger" and "broken-finger" mutants of F5 and F6 in mMTF-1 were characterized showed essentially no diminution of the ability of zinc to activate MREd binding in gel mobility shift assays, and in one case, appeared to have no effect on the zinc-induced transcriptional activation (*24*, *28*). Thus, the functional roles played by F5 and F6, under conditions of overexpression in mammalian cells, therefore remains unclear. In contrast, F1 (like F2, F3, and F4) have been shown to play important roles in functional activity of MTF-1, since broken-finger mutations deposited in F1, F2, F3, or F4 appeared to block MRE binding in vitro. A more recent report suggested that apo-F1 plays a negative regulatory role in modulating the MREd binding affinity of MTF-1; under conditions of low Zn(II), F1 contains no bound Zn(II) and physically occludes DNA binding by DNA-binding fingers F2, F3, and F4. When F1 is loaded with Zn(II), this negative repression is removed, and high affinity binding results (*28*). Deletion of F1 removes this negative regulation and creates a zinc-independent constitutive activator. These results make the prediction that F1 binds Zn(II) weakly, and its deletion would *not* be detrimental to high affinity MREd binding. Our pulsed alkylation experiments are not strongly supportive of either prediction. Although our results do suggest that reactivity of F1 can be distinguished from F2, F3, and F4, the effect is small; in fact, the alkylation rate constant for F1 thiolates is within a factor of 2 of that of the Sp1-zf zinc finger domains. This does not rule out a regulatory role for F1 based solely on differential affinity for Zn(II) since, in particular, it is not yet known how flanking regions might influence the Zn(II)-binding properties of individual zinc fingers. Furthermore, if recent studies from prokaryotic systems can be extended to mammalian cells, zinc homeostasis is not necessarily dictated by thermodynamic stability of metallo-regulatory zinc complexes and may well be under kinetic control (*53*). In any case, Zn(II)-loaded F1 clearly plays a critical role in stabilizing the protein−DNA complex. In fact, the affinity of MTF-zf26 is comparable to that of MTF-zf13 under the same solution conditions and may be indicative of essentially nonspecific binding (*27*). The implication of these results is that F1 and F4 play key roles in maintaining high affinity and specificity of binding by the zinc finger fragment of MTF-1. Further studies are required to better understand how and to what extent the zinc finger domain of intact MTF-1 mediates the zinc metalloregulation of MRE binding in vitro and transcriptional activation in mammalian cells in vivo.

## ACKNOWLEDGMENT

We thank Dr. Larry Dangott of the Protein Chemistry Laboratory at Texas A&M University for performing the N-terminal sequencing of recombinant MTF-zf26 and Professor Paul Fitzpatrick for helpful discussions.

## REFERENCES

1. Berg, J. M., and Shi, Y. (1996) *Science 271*, 1081−1085.
2. Vallee, B. L., and Fallchuk, K. H. (1993) *Physiol. Rev. 73*, 79−118.
3. Giedroc, D. P. (1994) in *Encyclopedia of Inorganic Chemistry* (King, R. B., Ed.) John Wiley & Sons, Ltd., Sussex, England.
4. Wolfe, S. A., Nekludova, L., and Pabo, C. O. (2000) *Annu. Rev. Biophys. Biomol. Struct. 29*, 183−212.
5. Luchinat, C., and Sola, M. (1994) in *Encyclopedia of Inorganic Chemistry* (King, R. B., Ed.) pp 4406−4434, John Wiley & Sons, Ltd., Sussex, England.
6. Thorp, H. H. (1998) *Chem. Biol. 5*, R125−R127.
7. Prince, R. H. (1994) in *Encyclopedia of Inorganic Chemistry* (King, R. B., ed.) pp 4434−4451, John Wiley & Sons, Ltd., Sussex, England.
8. Parkin G. (2000) *Chem. Commun. 20*, 1971−1985.
9. Outten, C. E., Outten, F. W., and O'Halloran, T. V. (1999) *J. Biol. Chem. 274*, 37517−37524.
10. Huckle, J. W., Morby, A. P., Turner, J. S., and Robinson, N. J. (1993) *Mol. Microbiol. 7*, 177−187.
11. Grotz, N., Fox, T., Connolly, E., Park, W., Guerinot, M. L., and Eide, D. (1998) *Proc. Natl. Acad. Sci. U.S.A. 95*, 7220−7224.
12. Andrews, G. K. (2000) *Biochem. Pharmacol. 59*, 95−104.
13. Westin, G., and Schaffner, W. (1988) *EMBO J. 7*, 3763−3770.
14. Brugnera, E., Georgiev, O., Radtke, F., Heuchel, R., Baker, E., Sutherland, G. R., and Schaffner, W. (1994) *Nucleic Acids Res. 22*, 3167−3173.
15. Stuart, G. W., Searle, P. F., and Palmiter, R. D. (1985) *Nature 317*, 828−831.
16. Günes, C., Heuchel, R., Georgiev, O., Müller, K.-H., Lichtlen, P., Blüthmann, H., Marino, S., Aguzzi, A., and Schaffner, W. (1998) *EMBO J. 17*, 2848−2854.
17. Heuchel, R., Radtke, F., Georgiev, O., Stark, G., Aguet, M., and Schaffner, W. (1994) *EMBO J. 13*, 2870−2875.
18. Palmiter, R. D., and Findley, S. D. (1995) *EMBO J. 14*, 639−649.
19. Langmade, S. J., Ravindra, R., Daniels, P. J., and Andrews, G. K. (2000) *J. Biol. Chem. 275*, 34803−34809.
20. Lichtlen, P., Wang, Y., Belser, T., Georgiev, O., Certa, U., Sack, R., and Schaffner, W. (2001) *Nucleic Acids Res. 29*, 1514−1523.
21. Radtke, F., Heuchel, R., Georgiev, O., Hergersberg, M., Gariglio, M., Dembic, Z., and Schaffner, W. (1993) *EMBO J. 12*, 1355−1362.
22. Chen, X., Agarwal, A., and Giedroc, D. P. (1998) *Biochemistry 37*, 11152−11161.

23. Radtke, F., Georgiev, O., Müller, H.-P., Brugnera, E., and Schaffner, W. (1995) *Nucleic Acids Res. 23*, 2277−2286.
24. Koizumi, S., Suzuki, K., Ogra, Y., Gong, P., and Otuska, F. (2000) *J. Cell. Physiol. 185*, 464−472.
25. Giedroc, D. P., Chen, X., and Apuy, J. L. (2001) *Antiox. Redox. Signal. 3*, 577−596.
26. Koizumi, S., Suzuki, K., Ogra, Y., Yamada, H., and Otsuka, F. (1999) *Eur. J. Biochem. 259*, 635−642.
27. Chen, X., Chu, M., and Giedroc, D. P. (1999) *Biochemistry 38*, 12915−12925.
28. Bittel, D. C., Smirnova, I. V., and Andrews, G. K. (2000) *J. Biol. Chem. 275*, 37194−37201.
29. Fabris D., Hathout Y., and Fenselau C. (1999) *Inorg. Chem. 38*, 1322−1325.
30. Wilker J. J., and Lippard S. J. (1997) *Inorg. Chem. 36*, 969−978.
31. Grapperhaus C. A., Tuntulani T., Reibenspies J. H., and Darensbourg M. Y. (1998) *Inorg. Chem. 37*, 4052−4058.
32. Suckau, D., Mak, M., and Przybylski, M. (1992) *Proc. Natl. Acad. Sci. U.S.A.* 89, 5630−5634.
33. Scaloni, A., Ferranti, P., De Simone, G., Mamone, G., Sannolo, N., and Malorni, A. (1999) *FEBS Lett. 452*, 190−204.
34. Fiedler, W., Borchers, C., Macht, M., Deininger, S. O., and Przybylski, M. (1998) *Bioconjugate Chem. 9*, 236−241.
35. Galvani, M., Hamdan, M., and Righetti, P. G. (2000) *Rapid Commun. Mass Spectrom. 14*, 1925−1931.
36. Basrur, V., Song, Y., Mazur, S. J., Higashimoto, Y., Turpin, J. A., Rice, W. G., Inman, J. K., and Appella, E. (2000) *J. Biol. Chem. 275*, 14890−14897.
37. Chertova, E. N., Kane, B. P., McGrath, C., Johnson, D. G., Sowder, R. C. I., Arthur, L. O., and Henderson, L. E. (1998) *Biochemistry 37*, 17890−17897.
38. Apuy, J. L., Park, Z.-Y., Swartz, P. D., Dangott, L. J., Russell, D. H., and Baldwin, T. O. (2002) *Biochemistry*, *41*, 15153−15163.
39. Guo, J., and Giedroc, D. P. (1997) *Biochemistry 36*, 730−742.
40. Kriwacki, R. W., Schultz, S. C., Steitz, T. A., and Caradonna, J. P. (1992) *Proc. Natl. Acad. Sci. U.S.A. 89*, 9759−9763.
41. Lundblad, R. J. (1991) in *Chemical Reagents for Protein Modification*, 2nd ed., pp 59−103, CRC Press, Boca Raton, FL.
42. Nicoli, M. Z., and Hastings, J. W. (1974) *J. Biol. Chem. 249*, 2393−2396.
43. Narayan, V. A., Kriwacki, R. W., and Caradonna, J. P. (1997) *J. Biol. Chem. 272*, 7801−7809.
44. Foster, M. P., Wuttke, D. S., Radhakrishnan, I., Case, D. A., Gottesfeld, J. M., and Wright, P. E. (1997) *Nat. Struct. Biol. 4*, 605−608.
45. Giedroc, D. P., Sinha, S. K., Brew, K., and Puett, D. (1985) *J. Biol. Chem. 260*, 13406−13413.
46. Berg, J. M. (1986) *Science 232*, 485−487.
47. Párraga, G., Horvath, S. J., Eisen, A., Taylor, W. E., Hood, L., Young, E. T., and Klevit, R. E. (1988) *Science 241*, 1489−1492.
48. Elrod-Erickson, M., Rould, M. A., Nekludova, L., and Pabo, C. O. (1996) *Structure 4*, 1171−1180.
49. Maynard A. T., and Covell D. G. (2001) *J. Am. Chem. Soc. 123*, 1047−1058.
50. Giedroc, D. P., Chen, X., Pennella, M., and LiWang, A. (2001) *J. Biol. Chem. 276*, in press.
51. Pavletich, N. P., and Pabo, C. O. (1993) *Science 261*, 1701−1707.
52. Uno, Y., Matsushita, K., Nagaoka, M., and Sugiura, Y. (2001) *Biochemistry 40*, 1787−1795.
53. Outten, C. E., and O'Halloran, T. V. (2001) *Science 292*, 2488−2492.

BI0112208